Enhanced light absorption in GaN/AlGaN midinfrared detectors and application for pixel-less upconversion imaging

L. K. Wu, H. L. Hao, and W. Z. Shen[a)]
Laboratory of Condensed Matter Spectroscopy and Opto-Electronic Physics, Department of Physics, Shanghai Jiao Tong University, 1954 Hua Shan Road, Shanghai 200030, China

(Received 28 October 2007; accepted 18 December 2007; published online 26 February 2008)

Based on the experimental responsivity of single-period GaN/AlGaN midinfrared (MIR) heterojunction interfacial work-function internal photoemission (HEIWIP) detectors, we have optimized in detail the single- and multiperiod GaN/AlGaN MIR HEIWIPs to enhance the light absorption in the detectors. The yielded parameters of emitter, intrinsic, and bottom contact layers could achieve large improvement of the MIR peak absorption efficiency in the multiperiod GaN/AlGaN MIR HEIWIPs. Employing the concept of photon frequency upconversion, we have further investigated the realization of MIR pixel-less upconversion imaging through the integration of GaN/AlGaN MIR HEIWIP with a GaN/AlGaN violet light-emitting diode (LED). Under the optimized device structures, good imaging characteristics and high upconversion efficiency could be expected in the GaN/AlGaN HEIWIP-LED MIR upconverter. © *2008 American Institute of Physics*. [DOI: 10.1063/1.2885121]

I. INTRODUCTION

Midinfrared (MIR) detection imaging has important applications in remote sensing technology, national defense, astronomy, and so on. The present MIR detection imaging is commonly achieved by expensive InSb or HgCdTe arrays with special hybrid readout circuits, while a low-cost MIR imaging device is not commercially available. The rapid progress in GaAs/AlGaAs quantum well infrared photodetectors (QWIPs) provides a price advantage for MIR detection, but the hybrid readout circuits are still needed to implement MIR imaging, so the cost remains high. To search for a low-cost MIR imaging technique, the concept of photon frequency upconversion, proposed and realized in Ge/GaAs heterojunction in the 1960s,[1] makes it possible to convert long wavelength radiation into short wavelength light, which could be directly detected by Si charge coupled devices (CCDs). Liu and co-workers,[2,3] have successfully demonstrated MIR upconversion imaging through the integration of GaAs/AlGaAs MIR QWIP with an InGaAs/GaAs near-infrared (NIR) light-emitting diode (LED). The basic mechanism of the MIR upconversion imaging is that under a forward constant bias, the MIR excitation decreases the QWIP resistance and then increases the potential drop across the NIR LED part, thus leading to an increase of NIR emission from LED, which falls in the effective imaging range of Si CCD. Therefore, the upconversion imaging from MIR to NIR could be realized. It should be pointed out that since the spatial distribution of incoming MIR radiation can be reproduced well in the photocurrent of QWIPs with sufficient number of periodic structures, this MIR upconversion imaging device is not necessarily separated into pixels,[4] which avoids the hybrid readout circuits and lowers the cost. However, due to the low responsivity of GaAs/AlGaAs QWIPs (Ref. 5) and extraction efficiency of LEDs, the upconversion efficiency of GaAs-based QWIP-LED is not high, usually about 1%–3%.[6]

With the breakthrough of growth techniques for the group-III nitride thin films, GaN-based system has attracted strong interest with the development in optical devices such as high-power transistors, ultraviolet photodetectors, blue lasers, and LEDs.[7] Recently, a novel GaN/AlGaN heterojunction interfacial work-function internal photoemission (HEIWIP) MIR photodetector has been demonstrated.[8] The main structure includes 200 nm Si-doped n^+-GaN emitter layer (5.0×10^{18} cm^{-3}), 600 nm AlGaN intrinsic layer (Al composition is 0.026), and 700 nm Si-doped n^+-GaN bottom contact layer (5.0×10^{18} cm^{-3}), as shown in the inset of Fig. 1(a). The GaN/AlGaN HEIWIP could detect 8–14 μm MIR light by utilizing the free carrier absorption in the GaN emitter layer, and ~0.5 A/W responsivity has been achieved in this unoptimized photodetector, comparable to that of optimized multiperiod GaAs/AlGaAs MIR QWIPs.[9] By optimizing the GaN/AlGaN MIR HEIWIP device structure to enhance the MIR absorption, the responsivity would be further improved, which opens ways to carry out high-efficiency MIR upconversion imaging via the integration of GaN/AlGaN MIR HEIWIP with a GaN/AlGaN violet LED.[10]

In this paper, according to the experimental responsivity of single GaN emitter/AlGaN intrinsic layer period HEIWIPs in Ref. 8, we have optimized in detail the single- and multiperiod GaN/AlGaN MIR HEIWIPs to achieve high MIR absorption efficiency. We have further studied the application of the GaN/AlGaN MIR HEIWIP to the pixel-less upconversion imaging device through the integration with a GaN/AlGaN violet LED. It is found that good contrast characteristic and high upconversion efficiency could be expected in this GaN/AlGaN HEIWIP-LED MIR upconverter.

[a)]Author to whom correspondence should be addressed. Electronic mail: wzshen@sjtu.edu.cn.

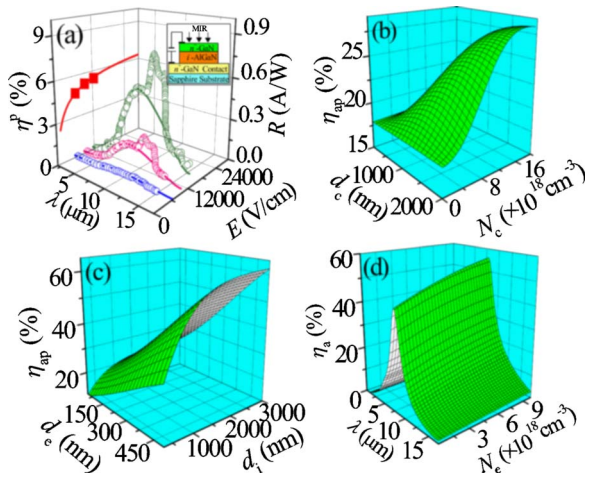

FIG. 1. (Color online) (a) Theoretical (solid curves) and experimental (open circles) responsivity R of single-period GaN/AlGaN MIR HEIWIP at different incoming wavelengths λ and electric fields E, together with the calculated (solid curve) and experimental (solid squares) peak quantum efficiency η^p under various E. The inset shows a schematic view of the single-period GaN/AlGaN MIR HEIWIP. Also presented are the dependences of peak absorption efficiency η_{ap} of single-period GaN/AlGaN MIR HEIWIP on (b) thickness d_c and doping concentration N_c of the bottom contact layer and (c) emitter layer thickness d_e and intrinsic layer thickness d_i, as well as the dependences of absorption efficiency η_a of single-period GaN/AlGaN MIR HEIWIP on (d) λ and doping concentration N_e of emitter layer.

II. LIGHT ABSORPTION IN HEIWIPS

A. Theory for light propagation

The detection mechanism for the GaN/AlGaN MIR HEIWIP shown in Fig. 1(a) is that under a certain bias, due to the free carrier absorption in the GaN emitter layer, the electrons are excited to the high energy states upon MIR radiation, followed by the internal photoemission of photoexcited carriers across the work function at the interfacial barrier resulting from the band offset of GaN and AlGaN, and then collected by the image force at the interface to generate photocurrent.[8] Here, we only consider the free carrier absorption process in the GaN/AlGaN MIR HEIWIP. To deal with the light propagation in the structure, we introduce the complex refractive index $\tilde{n}$ and complex permittivity $\tilde{\varepsilon}$ of the GaN layer according to the Drude model for free carrier after considering the contribution from phonons and plasmons:[11]

$$\tilde{n}^2 = \tilde{\varepsilon} = \varepsilon_\infty \left[1 + \frac{\omega_l^2 - \omega_t^2}{\omega_t^2 - \omega^2 - i\omega\Gamma} - \frac{\omega_p^2}{\omega(\omega + i\gamma)} \right], \tag{1}$$

where ε_∞ is the high frequency dielectric constant, ω_l, ω_t, and ω are the frequencies of longitudinal optical phonons, transverse optical (TO) phonons, and electromagnetic wave, respectively, Γ and γ are the damping constants of the phonon and plasmon, $\omega_p = \sqrt{4\pi n_e q^2/\varepsilon_\infty m^*}$ is the plasmon frequency of the free carrier with effective mass m^*, n_e is the free carrier concentration, and q is the magnitude of the electron charge. In the AlGaN layer the complex refractive index $\tilde{n}'$ and complex permittivity $\tilde{\varepsilon}'$ could be expressed as[12]

$$\tilde{n}'^2 = \tilde{\varepsilon}' = \varepsilon'_\infty + \sum_{k=1}^{2} \frac{S_k \omega_{t,k}^2}{\omega_{t,k}^2 - \omega^2 - i\omega\beta_k} - \frac{\varepsilon'_\infty \omega_p'^2}{\omega(\omega + i\gamma')}, \tag{2}$$

with ε'_∞ the high frequency dielectric constant, $\omega_{t,k}$ the GaN-like ($k=1$) and AlN-like ($k=2$) TO phonon frequencies, S_k the oscillator strength, β_k the broadening values of TO phonons, and γ' the phenomenological damping constant. The plasmon frequency in AlGaN, $\omega'_p = \sqrt{n'_e q^2/\varepsilon_0 \varepsilon'_\infty m^{*\prime}}$, is related to the vacuum permittivity ε_0, the free carrier concentration n'_e, and free carrier effective mass $m^{*\prime}$ in AlGaN. It should be noted that the above parameters for GaN and AlGaN are derived from Refs. 11 and 12 in the calculations.

We employ the transfer matrix method[13] to calculate the MIR photon absorption in the GaN/AlGaN MIR HEIWIP. Inside a multilayer semiconductor structure, the electrical vector in the medium is a superposition of the forward traveling field E^+ and the backward traveling field E^-. By using Maxwell equations and the boundary conditions for the electrical vector continuity on the surface between two layers with complex refractive indices $(\tilde{n}_j, \tilde{n}_{j+1})$, we can express the electric field at the jth layer in terms of the $(j+1)$th layer:

$$\begin{pmatrix} E_j^+ \\ E_j^- \end{pmatrix} = \frac{1}{2} \begin{pmatrix} [1 + \tilde{n}_{j+1}/\tilde{n}_j] e^{-i\delta_{j+1}} & [1 - \tilde{n}_{j+1}/\tilde{n}_j] e^{i\delta_{j+1}} \\ [1 - \tilde{n}_{j+1}/\tilde{n}_j] e^{-i\delta_{j+1}} & [1 + \tilde{n}_{j+1}/\tilde{n}_j] e^{i\delta_{j+1}} \end{pmatrix} \times \begin{pmatrix} E_{j+1}^+ \\ E_{j+1}^- \end{pmatrix} = C_j \begin{pmatrix} E_{j+1}^+ \\ E_{j+1}^- \end{pmatrix}, \tag{3}$$

where the subscript j denotes the layer order in the device structure, $\delta_{j+1} = 2\pi\tilde{n}_{j+1} d_{j+1}/\lambda_0$, with d_{j+1} the thickness of the $j+1$ layer, and λ_0 the wavelength in the vacuum. The light propagation from the top of the GaN/AlGaN MIR HEIWIP to the bottom could be described as

$$\begin{pmatrix} E_{\text{out}}^+ \\ E_{\text{out}}^- \end{pmatrix} = \prod C_j \begin{pmatrix} E_{\text{in}}^+ \\ E_{\text{in}}^- \end{pmatrix} = M \begin{pmatrix} E_{\text{in}}^+ \\ E_{\text{in}}^- \end{pmatrix}. \tag{4}$$

There is no return light at the bottom surface of the HEIWIP, and therefore, $E_{\text{out}}^- = 0$. Obviously, the physical quantities needed for the free carrier absorption calculations could be easily obtained through the transfer matrix M, such as the reflectance R and transmittance T of the whole structure. The total MIR absorption in the GaN/AlGaN HEIWIP is then determined as $A = 1 - R - T$.

B. Optimization of single-period GaN/AlGaN MIR HEIWIPs

According to the detection mechanism, the quantum efficiency η of GaN/AlGaN MIR HEIWIPs includes the MIR absorption efficiency η_a, internal photoemission efficiency η_i, and barrier collection efficiency η_c. Correspondingly, the responsivity R has the form

$$R = \frac{\eta g q \lambda}{hc} = \frac{\eta_a \eta_i \eta_c g q \lambda}{hc}. \tag{5}$$

Here g is the photoconductive gain, λ is the wavelength of incoming MIR light, h is the Planck constant, and c is the speed of light in vacuum. Describing the internal photoemission process by an escape cone model[14] and taking the form

of the barrier collection efficiency as in Ref. 15, we have simulated the responsivity of the single-period GaN/AlGaN MIR HEIWIP at several electric fields E, as shown in Fig. 1(a). The broad peak centered at ~12 μm in the experimental results (open circles) is due to the unintentionally introduced carbon impurities or nitrogen vacancies,[8] which is excluded from our theoretical considerations. The good agreement between the theoretical results (solids curves) and experimental data strongly demonstrates the free carrier absorption nature of the 8–14 μm response. Also shown is the calculated peak quantum efficiency η^p (λ=9 μm) as a function of E; the solid squares represent the experimental η^p.[8] We can see that η^p increases steeply in the small E range and then tends to saturation at high electric fields. It is noted that the calculated peak absorption efficiency is only ~20%, leaving much space for improvement, and therefore, it is necessary to enhance the MIR light absorption in the GaN/AlGaN HEIWIPs.

We first discuss the bottom contact layer to serve as a bottom mirror. Figure 1(b) shows the dependences of peak absorption efficiency η_{ap} on the thickness d_c and doping concentration N_c of the bottom contact layer. At small d_c, the MIR light could penetrate through the bottom contact layer, leading to insufficient absorption. With the increase of d_c, the thickness would be comparable to or surpass the penetration length of MIR radiation. More MIR light could be reflected back and reabsorbed by the emitter layer, so η_{ap} increases and then saturates with d_c. In the light doping bottom contact layer, the reflective index is small and η_{ap} is low. In the heavy doping case, the bottom contact layer functions as an effective bottom mirror and facilitates the absorption. In addition, the high doping concentration (~10^{19} cm^{-3}) guarantees reasonable Ohmic contact,[16] so d_c=1500 nm and N_c =1.5×10^{19} cm^{-3} would be appropriate parameters for the bottom contact layer.

One may recommend that the distributed Bragg reflector (DBR) is helpful as a bottom mirror to intensify MIR absorption in GaN/AlGaN HEIWIPs. In view of lattice matching, the GaN/$Al_xGa_{1-x}N$ DBR should be chosen. However, due to the low contrast of the refractive index between GaN and $Al_xGa_{1-x}N$, a large number of GaN/$Al_xGa_{1-x}N$ pairs or high AlN mole in $Al_xGa_{1-x}N$ is needed to provide high reflectivity, which would induce a lot of cracks during the DBR growth, damaging the performance of the DBR and disturbing the growth of the device structure above it.[17] Thus, the GaN/$Al_xGa_{1-x}N$ DBR is impractical here.

It is noticed that after the optimization of the bottom contact layer, η_{ap} shows an increase of ~10%. More improvement of absorption might be achieved through the optimization of emitter and intrinsic layers. Figure 1(c) displays the effects of GaN emitter layer thickness d_e and AlGaN intrinsic layer thickness d_i on η_{ap}. For the large d_e, the absorption will be effective in the emitter layer, and η_{ap} increases with d_e. It seems that we should choose an emitter layer as thick as possible; however, too large d_e is adverse to the internal photoemission efficiency;[18] d_e should not exceed the diffusion length of electrons (~250 nm). With the increase of d_i, the MIR light penetrates through the AlGaN intrinsic layer less easily, resulting in the enhancement of the

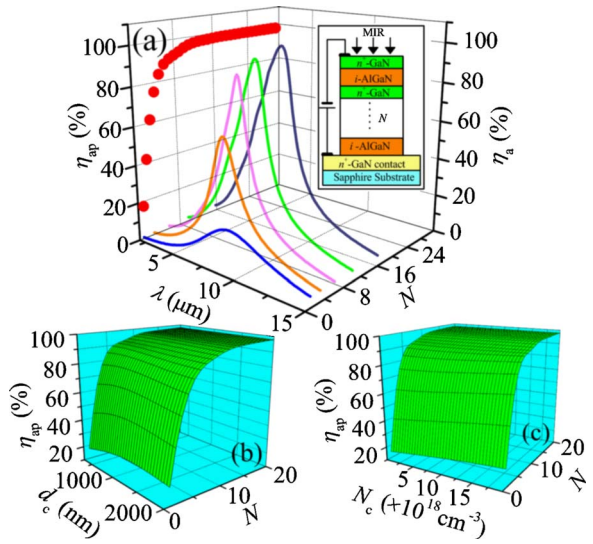

FIG. 2. (Color online) (a) Absorption efficiency η_a of GaN/AlGaN MIR HEIWIP under different incoming wavelengths λ and numbers of periods N, together with the peak absorption efficiency η_{ap} at various N. The inset illustrates the schematic structure of multiperiod GaN/AlGaN MIR HEIWIP. Also given is η_{ap} as functions of N at various (b) thicknesses d_c of the bottom contact layer and (c) doping concentration N_c of the bottom contact layer.

reflection at the interface between the emitter and intrinsic layers, which prompts the absorption in the emitter layer; so η_{ap} increases. When d_e is over ~1500 nm, the reflection at the interface saturates and the absorption tends to saturation. Figure 1(d) presents the relationship between η_a and λ at various concentrations N_e of the emitter layer. In the single-period GaN/AlGaN MIR HEIWIP, the detection wavelength due to free carrier absorption centers around 9 μm. With high N_e, there will be more carriers photoexcited in the emitter layer. Under the above optimized parameters, η_a increases with N_e slowly; we can set N_e=5.0×10^{18} cm^{-3}, the same as the doping concentration adopted in the experiment.[8] The present discussion yields the following parameters: d_c =1500 nm, N_c=1.5×10^{19} cm^{-3}, d_e=250 nm, d_i=1500 nm, and N_e=5.0×10^{18} cm^{-3}, where the absorption efficiency of the single-period GaN/AlGaN MIR HEIWIP could be ~50%, still leaving space for improvement.

C. Optimization of multiperiod GaN/AlGaN MIR HEIWIPs

Following the analysis for single-period GaN/AlGaN MIR HEIWIPs, we have investigated the HEIWIPs with multiple periods of GaN emitter/AlGaN intrinsic layers to realize more MIR absorption, the schematic diagram of which is shown as the inset in Fig. 2(a). We have calculated η_a of the multiperiod GaN/AlGaN MIR HEIWIP as functions of period number N and λ, illustrated by Fig. 2(a). With the increase of N, the MIR absorption intensifies. Nevertheless, in order to sustain the impact ionization process in the detector, the number of periodic structures cannot be increased infinitely. The dependence of N on the device parameters could be expressed as $2^{N-2}q^2d_i \leq \varepsilon_0 \Delta A$,[19] with Δ the ionization barrier (~31 meV) and A the optical window area. Theoretical estimation with these parameters yields N

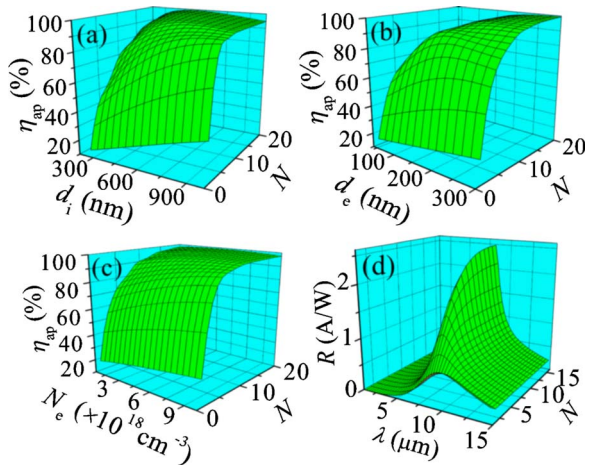

FIG. 3. (Color online) Relationship between peak absorption efficiency η_{ap} and number of periods N under different (a) intrinsic layer thicknesses d_i, (b) emitter layer thicknesses d_e, and (c) doping concentrations N_e in the emitter layer. Also shown is the responsivity of GaN/AlGaN MIR HEIWIP at various (d) incoming wavelengths λ and N.

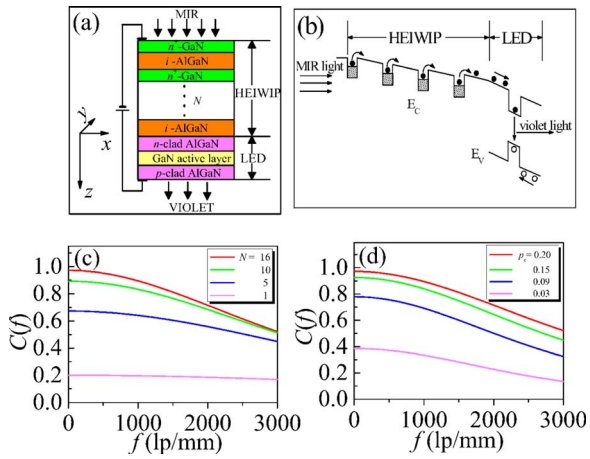

FIG. 4. (Color online) (a) Schematic structure of GaN/AlGaN HEIWIP-LED upconverter, (b) band diagram of GaN/AlGaN HEIWIP-LED upconverter under operating condition, (c) spatial frequency f dependence of contrast transfer characteristic $C(f)$ at different numbers of periods N, and (d) spatial frequency f dependence of $C(f)$ at different capture probabilities p_c.

$\leqslant 16$ as a limit. It is also seen that the absorption center of the multiperiod GaN/AlGaN MIR HEIWIP shows a slight blueshift (from about 9 to 8 μm) with the increase of N. Since the skin depth decreases rapidly with increasing λ, the absorption of short wavelength will be enhanced faster with N than that of long wavelength in the free carrier response range (8–14 μm), which compensates the cavity effect[20] and leads to the slight blueshift of the absorption peak. Together shown is η_{ap} as a function of N, which increases steeply with N and then tends to saturation. In fact, when the number of periodic structures surpasses 8, we can expect over 90% peak absorption efficiency in the multiperiod GaN/AlGaN MIR HEIWIP. In the following, we would present the detailed device optimization of the multiperiod GaN/AlGaN MIR HEIWIP.

Figures 2(b) and 2(c) display the effect of the bottom contact layer parameters (d_c and N_c) on η_{ap}. For the multiperiod GaN/AlGaN MIR HEIWIP with small N, due to the effective reflection of the bottom contact layer, η_{ap} changes with d_c and N_c as that in the single-period GaN/AlGaN MIR HEIWIP case. However, with the large number of periodic structures in the GaN/AlGaN HEIWIP, η_{ap} is not influenced much by d_c and N_c. Since with large N little MIR radiation could reach the bottom contact layer and η_{ap} is insensitive to the parameters of the bottom contact layer, it is not necessary for d_c in multiperiod GaN/AlGaN MIR HEIWIPs to be as thick as that in the single-period one; we can adopt $d_c = 700$ nm as in Ref. 8 and $N_c = 1.5 \times 10^{19}$ cm^{-3} for Ohmic contact.

Now, we study the parameters of the emitter and intrinsic layers. Figure 3(a) demonstrates that at small N, η_{ap} increases with d_i. The MIR light could not penetrate through the intrinsic layers easily under large d_i. The reflection is significant at the interfaces. As a result, the MIR radiation absorption is enhanced in the emitter layers. With the increase of N, there are more emitter layers contributing to the MIR absorption, η_{ap} could be high enough that even the MIR light penetrates through the intrinsic layers, a thick intrinsic layer is not necessary, and η_{ap} will saturate at certain values of d_i. Figures 3(b) and 3(c) show the change of η_{ap} with N at different d_e and N_e. In the small N range, η_{ap} increases with d_e and N_e. Under the large N, η_{ap} first increases with d_e and then saturates; at the same time, η_{ap} does not show any obvious dependence on N_e. This is due to the fact that at large N, the sufficient number of emitter layers can compensate the requirement of a thick emitter layer and high N_e to realize sufficient absorption.

The above analysis indicates that with the following parameters: $d_c = 700$ nm, $N_c = 1.5 \times 10^{19}$ cm^{-3}, $d_i = 600$ nm, $d_e = 200$ nm, and $N_e = 5.0 \times 10^{18}$ cm^{-3}, we can achieve much improved MIR absorption in multiperiod GaN/AlGaN HEIWIPs. Under these optimized parameters, the responsivity of multiperiod GaN/AlGaN MIR HEIWIPs has been calculated, as shown in Fig. 3(d). Compared to the GaAs/AlGaAs QWIP, which has a responsivity of only 0.01–0.03 A/W,[5] the multiperiod GaN/AlGaN HEIWIP is more sensitive to the MIR radiation, showing the good response characteristic for application to the upconversion imaging device discussed in Sec. III. Moreover, we point out that in contrast with the optimized layer thicknesses of the single-period GaN/AlGaN MIR HEIWIP, those in the multiperiod one are thinner, which ensures that the response time of the GaN/AlGaN MIR HEIWIP would not be extended much even with multiple periods.

III. HEIWIPS FOR UPCONVERSION IMAGING

A. Photocurrent from HEIWIPs

Integrating the GaN/AlGaN MIR HEIWIP with a GaN/AlGaN violet LED, we can carry out the photon frequency upconversion from MIR to violet light and implement the detection imaging through Si CCD. The schematic structure of the GaN/AlGaN HEIWIP-LED upconverter is shown in Fig. 4(a). At the same time, the band diagram of the HEIWIP-LED upconverter under operating condition is illustrated by Fig. 4(b), where the electrons are represented by solid circles and holes by open circles, E_C is the conduction

band, and E_V indicates the valence band. Under the biasing condition and upon MIR radiation, electrons are photoexcited from the low energy states to the high ones of the conduction band in the GaN emitter layers, followed by internal photoemission of photoexcited electrons across the interfacial barrier, and are collected by the image force to generate photocurrent. The photoexcited electrons past the HEIWIP are injected into the LED active layer and then they recombine with the holes from the *p*-clad layer, leading to the emission of violet light through the radiative recombination, which falls in the effective detection range of Si CCD. Thus, the upconversion imaging from MIR to violet radiation is realized.

Employing the spectral decomposition approach, we can express the radiation photon flux distribution of a two-dimensional sine target as $\phi^{\text{in}}=\phi_0^{\text{in}}+\phi_{\vec{f}}^{\text{in}}\cos 2\pi\vec{f}\vec{r}$, with $\vec{r}=(x,y)$, ϕ_0^{in} the average photon flux of the incoming MIR radiation, f the spatial frequency (reciprocal of the spatial period of a sine target), and $\phi_{\vec{f}}^{\text{in}}$ the signal part amplitude of the sine wave. We assume that the in-plane potential is uniform within the emitter layers. The carrier transport along the z axis drifts with a constant velocity and neglects the thermal emission of carriers (the working temperature of GaN/AlGaN MIR HEIWIPs is ~5.3 K). Starting from the current continuity equation of the carrier transport in the GaN/AlGaN MIR HEIWIP, we can get the average photocurrent density j_0 over the planes:[18]

$$j_0=\frac{qG\phi_0^{\text{in}}}{p_c}, \tag{6}$$

and the signal photocurrent density part $j_{\vec{f}}$ reaching the GaN/AlGaN violet LED:

$$j_{\vec{f}}=qG\phi_{\vec{f}}^{\text{in}}\exp(-4\pi^2l^2f^2)\frac{1-(1-p_c)^N\exp(-4\pi^2l^2f^2N)}{1-(1-p_c)\exp(-4\pi^2l^2f^2)}. \tag{7}$$

Here G is the ratio of photocarriers across the interfacial barriers, l is the characteristic diffusion length, and p_c is the carrier capture probability.[21]

B. Contrast transfer characteristic

To investigate the figure of merit of the GaN/AlGaN MIR HEIWIP in the upconversion imaging device, we study the contrast transfer characteristic $C(f)$ of the GaN/AlGaN MIR HEIWIP, which is the ratio of the photocurrent contrast $(j_{\vec{f}}/j_0)$ to the object contrast $(\phi_{\vec{f}}^{\text{in}}/\phi_0^{\text{in}})$ and indicates the ability of GaN/AlGaN HEIWIP to maintain the spatial distribution of MIR radiation. From Eqs. (6) and (7), we can get easily

$$C(f)=\frac{j_{\vec{f}}/j_0}{\phi_{\vec{f}}^{\text{in}}/\phi_0^{\text{in}}}=p_c\exp(-4\pi^2l^2f^2)\times\frac{1-(1-p_c)^N\exp(-4\pi^2l^2f^2N)}{1-(1-p_c)\exp(-4\pi^2l^2f^2)}. \tag{8}$$

Clearly, $C(f)$ relates closely to N and p_c. We have calculated the relationships among them at different spatial frequencies, as shown in Figs. 4(c) and 4(d). From Fig. 4(c), it can be seen that $C(f)$ increases with N, indicating that the object contrast can be transferred better through the photocurrent with the larger N. On the other hand, the spatial distribution of the incoming MIR light can be reproduced well in the photocurrent density driving the GaN/AlGaN violet LED for the GaN/AlGaN HEIWIP with sufficient number of periodic structures, and then the GaN/AlGaN HEIWIP-LED upconverter is not necessarily separated into pixels.[4] Considering the discussion for the limitation of N in Sec. II C, $N=16$ would be preferred for the multiperiod GaN/AlGaN MIR HEIWIP to implement pixel-less upconversion imaging. We note that due to the diffraction limit, the total active part of the GaN/AlGaN HEIWIP-LED should not be thicker than the MIR wavelength in order to get an image with negligible distortion.[2] For the incoming 8 μm MIR light, the active segment of 16-period GaN/AlGaN MIR HEIWIP and GaN/AlGaN violet LED could meet the requirement. Figure 4(d) displays the effect of p_c on $C(f)$; $C(f)$ is higher for the larger p_c. By analyzing Eqs. (6) and (7), we know that with the increase of p_c, the uniform photocurrent part will decrease faster than its nonuniform counterpart; the object contrast is then efficiently transferred. Also, the dependence of $C(f)$ on p_c is not so significant for the large value of p_c, and we could get satisfying contrast transfer characteristic for $p_c=0.2$. Nevertheless, p_c is not a quantity correlating directly with the practical device design, and we should try to find the physical quantities influencing p_c.

In fact, p_c is relevant with the photoconductive gain of the GaN/AlGaN MIR HEIWIP. The relationship between them could be described as[21]

$$g=\frac{1-p_c}{Np_c}. \tag{9}$$

Furthermore, according to the analysis of the detector intrinsic time response,[22] the current responsivity ties to the electric field E by

$$R=\frac{3\eta q\mu\tau E}{2NwkT_0}, \tag{10}$$

where μ is the mobility of electrons, τ is the energy relaxation time of the hot electrons, $w=d_e+d_i$ is the thickness of the GaN emitter/AlGaN intrinsic layer period, k is Boltzmann's constant, and T_0 is the working temperature of GaN/AlGaN MIR HEIWIPs. Substituting Eq. (9) into Eq. (5) and using Eq. (10), we could obtain

$$p_c=\left(1+\frac{3\mu\tau Ehc}{2wkT_0\lambda}\right)^{-1}. \tag{11}$$

We have further investigated the effects of E and w on p_c, as demonstrated in Fig. 5. Under the weak electric field, the hot electrons pass the GaN/AlGaN MIR HEIWIP slowly, resulting in the large possibility to be captured, so p_c increases with the decrease of E. The quantum efficiency of GaN/AlGaN MIR HEIWIP is not high at low electric field

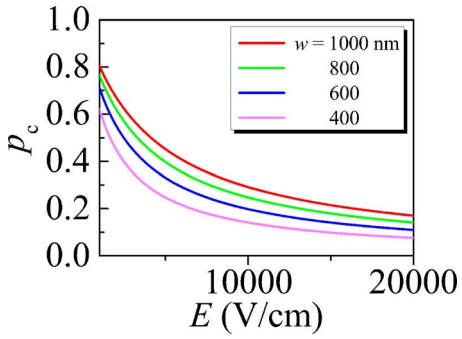

FIG. 5. (Color online) p_c as a function of electric field E under various GaN emitter/AlGaN intrinsic layer period thicknesses w.

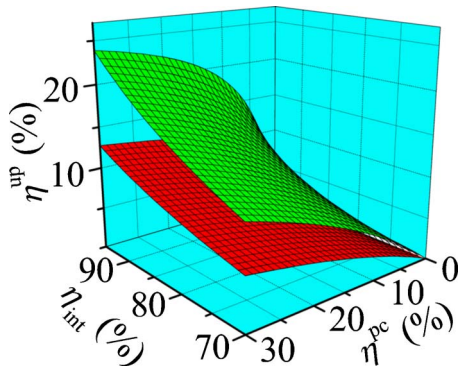

FIG. 6. (Color online) Upconversion efficiency η^{up} of GaN/AlGaN HEIWIP-LED (top) and GaAs/AlGaAs QWIP-LED (bottom) as functions of LED internal quantum efficiency η_{int} and extraction efficiency η^{pc}.

due to the low collection efficiency, as illustrated in Fig. 1(a). The optimal value of p_c should be a trade-off between good contrast transfer characteristic and high quantum efficiency. In addition, since the hot carriers will spend more time passing through the emitter/intrinsic layer period with large w, they will have a high probability to be captured, and p_c increases with w. However, large w might increase the response time of the GaN/AlGaN MIR HEIWIP, which is not appreciated. Taking into account that the satisfying contrast transfer characteristic of HEIWIPs could be achieved at $p_c = 0.2$, we can select $N=16$, $E=13\,000$ V/cm, and $w=800$ nm as suitable parameters for the application of GaN/AlGaN MIR HEIWIPs to the pixel-less upconversion imaging device.

We also note that the lateral diffusion of current is adverse to the imaging characteristics. During the transport of the photocarriers to the LED, the lateral diffusion length of the photocarrier has the form $l=\sqrt{DNw/v}$, where D is the lateral diffusion coefficient and v is the drift velocity of the photocarriers. For the detector with $D=0.1-0.3$ cm^2/s, $N=16$, $w=800$ nm, and $v\sim10^6$ cm/s; the lateral diffusion length of the photocarriers reaching the LED is in the range of <1 μm, far less than the MIR wavelength (8 μm). Therefore, according to the diffraction limit, the lateral diffusion of current in the present upconverter structure is negligible in practice, which would not induce obvious distortion and smearing of the MIR image.

C. Upconversion efficiency

Upconversion efficiency η^{up} is the ratio of violet photon flux to the incoming MIR one, denoting how efficiently the MIR radiation is converted into violet light. Using the carrier diffusion equation in the LED active region and considering the photon recycling process,[23] we could obtain the relationship between the output violet light photon flux and photocurrent density; the detailed analysis can be found in Ref. 24. By using Eqs. (6) and (7), we can derive the upconversion efficiency of GaN/AlGaN HEIWIP-LED. Figure 6 shows η^{up} of GaN/AlGaN HEIWIP-LED and GaAs/AlGaAs QWIP-LED as functions of internal quantum efficiency η_{int} and photon extraction efficiency η^{pc} of GaN/AlGaN violet LED. For the high η_{int}, the hot carriers recombine effectively in the GaN active layer of LED, leading to the generation of more violet photons and benefiting the η^{pc}. Generally, η_{int} could reach over 90% by reducing the nonradiative recombination process.[23] In normal LEDs, due to the internal total reflection, the photons generated in the active region have small a probability to escape the LED; η^{pc} is not high ($\sim$2% in GaAs/AlGaAs and $\sim$5% in GaN/AlGaN LEDs). Nevertheless, large η^{up} is required to provide sufficient violet photons detected by Si CCD in the upconverter. We have predicted that η^{up} could be achieved over 20% in the powerful resonant-enhanced LEDs.[24] At the same time, the existence of a resonant cavity guarantees negligible cross-talk resulting from the leaked violet photons from the GaN/AlGaN LED reabsorbed by the emitter layers of GaN/AlGaN MIR HEIWIPs.

It should be noted that, although the material quality of GaN at present is not as good as that of GaAs, there will be much defects generated in GaN thin film during the growth; however, the diffusion length of electrons in GaN is significantly larger than that in GaAs. The light absorption efficiency increases with the thickness of the emitter layer until the thickness is larger than the diffusion length, where only a fraction of electrons contributes to the output current density; therefore, the light absorption efficiency tends to saturation due to the lost of electrons in the diffusion. This allows us to fabricate GaN-based photodetector with a much thicker emitter layer than its GaAs counterpart, and the higher light absorption efficiency in GaN HEIWIP detector can be realized. As a result, we can expect that the upconversion efficiency of GaN/AlGaN HEIWIP-LED is higher than that of GaAs/AlGaAs QWIP-LED. All of these show that the optimal multiperiod GaN/AlGaN MIR HEIWIPs have significant potential application in the MIR pixel-less upconversion imaging.

IV. SUMMARY AND CONCLUSION

We have investigated the enhancement of free carrier absorption in the single- and multiperiod GaN/AlGaN MIR HEIWIPs on the basis of the responsivity simulations for the single-period case. Employing the transfer matrix method to deal with MIR absorption in the detectors, we have yielded the optimized thicknesses of the emitter, intrinsic, and bottom contact layers, as well as the doping concentrations of the emitter and bottom contact layers. We have found that under the optimized device parameters, over 90% peak ab-

sorption efficiency can be expected in the GaN/AlGaN MIR HEIWIP with more than eight periods. By integrating the GaN/AlGaN MIR HEIWIP with a GaN/AlGaN violet LED, we have studied the MIR pixel-less upconversion imaging in this GaN-based HEIWIP-LED upconverter. Through the analysis of the contrast transfer characteristic for the detector, we choose a 16-period GaN/AlGaN HEIWIP to serve as the detector segment to implement MIR pixel-less upconversion imaging, where we could also achieve high upconversion efficiency in the optimized GaN/AlGaN HEIWIP-LED MIR upconverter.

ACKNOWLEDGMENTS

This work was supported by the National Natural Science Foundation of China under Contract No. 60576067, the Shanghai Municipal Commission of Science and Technology Project of 05QMH1411, and the National Minister of Education Program for Changjiang Scholars and Innovative Research Team in University (PCSIRT).

[1]P. W. Kruse, F. C. Pribble, and R. G. Schulze, J. Appl. Phys. **38**, 1718 (1967).
[2]H. C. Liu, J. Li, Z. R. Wasilewski, and M. Buchanan, Electron. Lett. **31**, 832 (1995).
[3]L. B. Allard, H. C. Liu, M. Buchanan, and Z. R. Wasilewski, Appl. Phys. Lett. **70**, 2784 (1997).
[4]V. Ryzhii, H. C. Liu, I. Khmyrova, and M. Ryzhii, IEEE J. Quantum Electron. **33**, 1527 (1997).
[5]E. Dupont, H. C. Liu, M. Buchanan, Z. R. Wasilewski, D. St-Germain, and P. Chevrette, Appl. Phys. Lett. **75**, 563 (1999).
[6]E. Dupont, M. Byloos, M. Gao, M. Buchanan, C.-Y. Song, Z. R. Wasilewski, and H. C. Liu, IEEE Photonics Technol. Lett. **14**, 182 (2002).
[7]S. Nakamura and G. Fasol, *The Blue Laser Diode: GaN Based Light Emitters and Lasers* (Springer-Verlag, New York, 1997).
[8]G. Ariyawansa, M. B. M. Rinzan, M. Strassburg, N. Dietz, A. G. U. Perera, S. G. Matsik, A. Asghar, I. T. Ferguson, H. Luo, and H. C. Liu, Appl. Phys. Lett. **89**, 141122 (2006).
[9]B. F. Levine, J. Appl. Phys. **74**, R1 (1993).
[10]L. K. Wu, H. L. Hao, W. Z. Shen, G. Ariyawansa, A. G. U. Perera, and S. G. Matsik, Opt. Lett. **32**, 2366 (2007).
[11]T. Kozawa, T. Kachi, H. Kano, Y. Taga, M. Hashimoto, N. Koide, and K. Manabe, J. Appl. Phys. **75**, 1098 (1994).
[12]Z. G. Hu, M. Strassburg, N. Dietz, A. G. U. Perera, A. Asghar, and I. T. Ferguson, Phys. Rev. B **72**, 245326 (2005).
[13]Z. Knittl, *Optics of Thin Films* (Wiley, London, 1976).
[14]R. Williams, *Semiconductors and Semimetals* (Academic, New York, 1970).
[15]J. M. Mooney, J. Appl. Phys. **65**, 2869 (1989).
[16]S. J. Pearton, J. C. Zolper, R. J. Shul, and F. Ren, J. Appl. Phys. **86**, 1 (1999).
[17]N. Nakada, H. Ishikawa, T. Egawa, and T. Jimbo, Jpn. J. Appl. Phys., Part 2 **42**, L144 (2003).
[18]L. K. Wu and W. Z. Shen, J. Appl. Phys. **100**, 044508 (2006).
[19]W. Z. Shen, A. G. U. Perera, H. C. Liu, M. Buchanan, and W. J. Schaff, Appl. Phys. Lett. **71**, 2677 (1997).
[20]D. G. Esaev, S. G. Matsik, M. B. M. Rinzan, A. G. U. Perera, H. C. Liu, and M. Buchanan, J. Appl. Phys. **93**, 1879 (2003).
[21]H. C. Liu, Appl. Phys. Lett. **60**, 1507 (1992).
[22]W. Z. Shen and A. G. U. Perera, Infrared Phys. Technol. **39**, 329 (1998).
[23]I. Schnitzer, E. Yablonovitch, C. Caneau, and T. J. Gmitter, Appl. Phys. Lett. **62**, 131 (1993).
[24]L. K. Wu and W. Z. Shen, IEEE J. Quantum Electron. **43**, 411 (2007).